Friedrich-Alexander-Universität
Erlangen-Nürnberg

Advanced Laboratory Course

M48: Properties of the Z^0-Boson [EN]

Authors:

Saurabh Gangwar saurabh.gangwar@fau.de
Alexander Kulyabin alexander.kulyabin@fau.de

Group M575 ♣

2023 – Summer Semester

Contents

1 Preparation

1.1 Abstract

In this lab we deal with data of collision of collision of positron es and electrons from the collider, which is related to Z^0 boson theory. By separating the final events with simulation-designed selection criteria and finding the cross sections we obtain some of Z^0-boson properties. In additional, we determine the number of light neutrinos in the process.

Below we briefly describe the theory and the essence of the experiment, relying mainly on [1].

1.2 Theory

1.2.1 Standart model

The basic and most successful model in particle physics is Standard Model. It descirbes all known fundamental forces except gravity - weak, strong and electromagnetic intersections, and contains and classify all known particles.

In this model, all substances consist of particle s with spin 1/2. Of these, six are the so-called leptons - electron, muon, tauon, mu neutrino, tau neutrino, electron neutrino, other six, so-called quarks - u,d,s,c,b,t. There are 12 more antiparticles corresponding to these 12 particles.

The particles that carry the strong interaction are 8 gluons. The quantum of electromagnetic interaction is photon. The carriers of the weak interaction are W^+, W^-, Z^0 - bosons.

Also in the theory there is Higgs particle, the field of which is responsible for the appearance of masses.

On the figure below one can find all these particles with their spin, mass and electromagnetic charge.

Quarks are subject to all interactions. Electron, muon, taon interact with weak and electromagnetic forces. All neutrinos are subject only to weak interaction. For more details see [2].

1.2.2 Cross section and decay width

One of the most important concepts in elementary particle physics, when considering reactions with two initial particles, is the scattering cross section.

Consider a target with particles under a stream of particles of a different type. The particles can interact with each other with some probability. Definition of the cross section:

$$\sigma = \frac{\text{number of interactions per time and per target particle number}}{\text{incoming particle flux}} \tag{1}$$

It can be also written (for enough large time of detection) as

$$\sigma = \frac{N}{\int \mathcal{L} dt}, \tag{2}$$

where N is the number during the time and $\int \mathcal{L} dt$ is integrated luminosity during this time, according to [1].

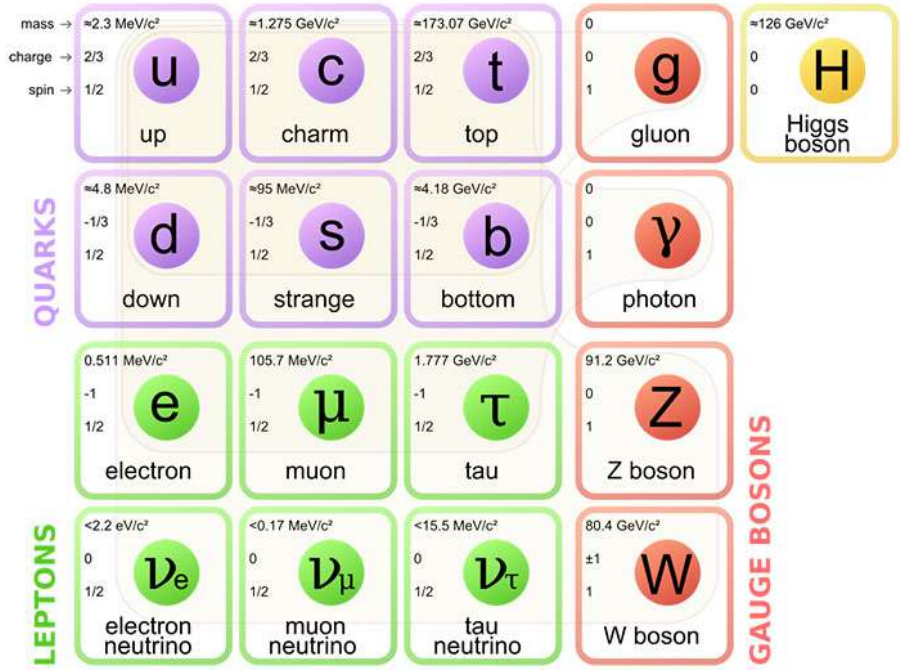

Figure 1: Particles of Standart Model, taken from [2].

Moreover, important concept is the differential scattering cross section, $d\sigma$, corresponding to the number N only for events in which particles hit the target at a certain solid angle $d\Omega$ and angles (θ, ϕ). The integrated value corresponds to the definition above and also is called the total scattering cross section:

$$\sigma = \int_{\Omega} d\Omega \frac{d\sigma}{d\Omega} \tag{3}$$

The width of the decay can be defined as (for enough large time of detection):

$$\Gamma = \hbar \frac{\text{probability of the decay during the time } t}{t} \tag{4}$$

Life time of the particle:

$$\tau = \frac{\hbar}{\Gamma} \tag{5}$$

The cross section and decay width can be calculated using the model and Quantum Field Theory framework.

1.2.3 Electroweak interaction

As told in [1], at first the gauge theory of weak interaction was based on $SU(2)$ group and includes $W^{\pm}$-bosons and coupling constant g. The Fermi constant:

$$G_F = \frac{\sqrt{2} g^2}{8 M_{W^{\pm}}^2} = 1.16637 \times 10^{-5} \text{GeV}^{-2} \tag{6}$$

Here $M_{W^{\pm}}$ are $W^{\pm}$-bosons masses. To expand the symmetry including photon, $U(1)$ gauge group and Y^0 particle was introduced in Standrat Model. Then, the photon is given as a linear

combination:

$$|\gamma\rangle = \cos\theta_W \left|Y^0\right\rangle + \sin\theta_W \left|W^0\right\rangle \tag{7}$$

And Z^0:

$$\left|Z^0\right\rangle = -\sin\theta_W \left|Y^0\right\rangle + \cos\theta_W \left|W^0\right\rangle \tag{8}$$

Here θ_W is so-called Weinberg angel, satisfying the relations:

$$\sin^2\theta_W = \frac{e^2}{g^2} \tag{9}$$

$$\cos\theta_W = \frac{M_{W^\pm}}{M_{Z^0}} \tag{10}$$

It is also important to note again that in the Standard Model all bosons are in fact massless. The masses appear due to the Higgs mechanism, being in fact the parameters of the potential of the Higgs scalar field.

1.2.4 Fragmentation

Although our lab work is mainly concerned with electroweak interactions, the strong interaction effect also plays a role. Let us briefly describe the essence here, following [1].

QCD, part of the Standart Model, is gauge theory of strong interactiones. It corresponds to the color charge (red, green, blue) of the quarks, particles participating in this interaction. The symmetry is $SU(3)$.

QCD coupling constant, taking into account the dependence on renormalisation scale:

$$\alpha_s(q^2) = \frac{12\pi}{(33 - 2N_f)\log(q^2/\Lambda^2)} \tag{11}$$

N_f is number of quark types (or so-called flavour) involved at the energy level of the process.

The fragmentation effect is, rougly speaking when quark and anti-quark flies apart and anti-quark pairs born in strong QCD fields between them. And, in particular, this effect occurs after the collision and reaction of an electron with a positron, see the figure.

1.2.5 Z^0 resonance and related

We consider e^+e^- collision, which can lead to several different variants.

First is Bhabha scattering.

Second is turning into different fermion anti-fermion pair ($e^+e^- \to \bar{f}f$) throw virtual photon or Z^0 boson.

Third is inelastic scattering with two virtual photons.

And the last is annigilation and turning into photons.

We are interested in reactions involving the Z^0-boson. Its main parameters are decay widths (to different states) and mass. Total decay width (the indices mean the corresponding fermions at the end, Γ_ν is meant for single of the N_ν possible type pairs, while Γ_{unknown} corresponds to unknown decays, there is no reason to consider it nonzero):

$$\Gamma_Z = \Gamma_{\text{e}} + \Gamma_\mu + \Gamma_\tau + \Gamma_{\text{had}} + N_\nu\Gamma_\nu + \Gamma_{\text{unknown}} \tag{12}$$

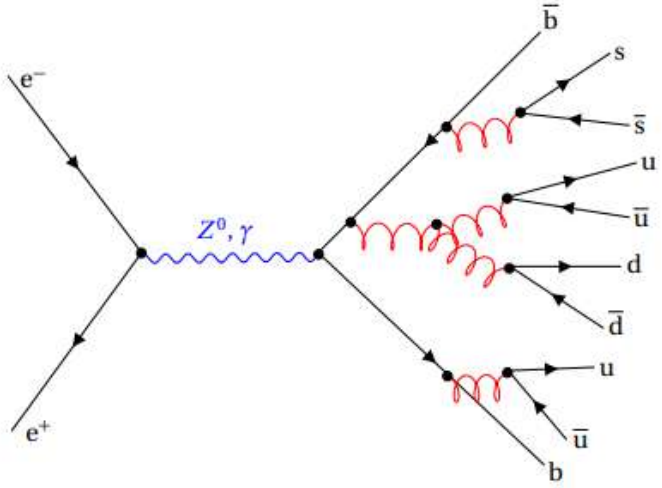

Figure 2: Fragmentation after the reaction, taken from [1].

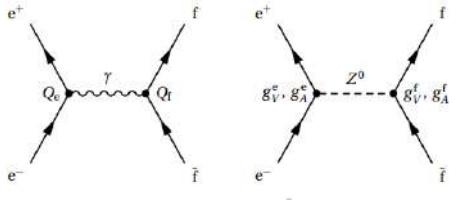

Figure 3: $e^+e^- \to \bar{f}f$ (s channel). g_V are corresponding vector couplings, g_A - axial vector couplings, Q - electrical charges. Taken from [1].

The lowest order Feynman diagram for $e^+e^- \to \bar{f}f$, so-called s channel, can bee seen on the figure.

Decay width of Z boson decay into two Fermions is given by

$$\Gamma_f = \frac{N_c^f \cdot \sqrt{2}}{12\pi} \cdot G_F \cdot M_{Z^0}^3 \cdot \left(\left(g_V^f\right)^2 + \left(g_A^f\right)^2 \right), \tag{13}$$

where N_c^f is colour factor (1 for leptons, 3 for quarks), $g_V^f = I_3^f - 2Q_f \sin^2\theta_W$, $g_A^f = I_3^f$, Q_f -charge of the fermions, I_3^f - weak charge.

Cross section of $e^+e^- \to \bar{f}f$, neglecting photon diagramm:

$$\sigma_f = \frac{12\pi\Gamma_e\Gamma_f}{sM_Z^2} \cdot |Z_0 \,\text{propagator}\,|^2 = \frac{12\pi}{M_{Z^0}^2} \cdot \frac{s\Gamma_e\Gamma_f}{\left(s - M_{Z^0}^2\right)^2 + \left(s^2\Gamma_Z^2/M_{Z^0}^2\right)} \tag{14}$$

At the energy scale close to the Z^0-boson mass, a resonance peak of the cross section is observed:

$$\sigma_f^{peak} = \frac{12\pi}{M_{Z^0}^2} \frac{\Gamma_e}{\Gamma_Z} \frac{\Gamma_f}{\Gamma_Z} \tag{15}$$

Using the data about decay widths (see the figure), one could can calculate the following quantities:

Channel	Partial width
$\Gamma_e = \Gamma_\mu = \Gamma_\tau = \Gamma_\ell$	83.8 MeV
$\Gamma_{\nu_e} = \Gamma_{\nu_\mu} = \Gamma_{\nu_\tau} = \Gamma_\nu$	167.6 MeV
$\Gamma_u = \Gamma_c$	299 MeV
$\Gamma_d = \Gamma_s = \Gamma_b$	378 MeV

Figure 4: Decay widths. [1]

$$\Gamma_{had} = 3\Gamma_b + 2\Gamma_c = 1732\text{MeV} \tag{16}$$

$$\Gamma_{charged} = 3\Gamma_l = 251.4\text{MeV} \tag{17}$$

$$\Gamma_{invis} = 3\Gamma_\nu = 502.8\text{MeV} \tag{18}$$

Total decay width:

$$\Gamma_Z = \Gamma_{had} + \Gamma_{charged} + \Gamma_{invis} = 2486.2\text{MeV} \tag{19}$$

Life time:

$$\tau = \frac{\hbar}{\Gamma_Z} \approx 2.6475 \times 10^{-25}\text{s} \tag{20}$$

Then, for peak cross sections we get (using [3] data for the Z^0 mass):

$$\sigma_{had}^{peak} 41.4\text{nb}\,,\ \sigma_f^{peak} \approx 22.2\text{nb} \tag{21}$$

In addition to the above diagrams, $e^+e^- \to \bar{f}f$ has the contribution of the mentioned Bhabha scattering. Its lowest order Feynman diagram, so-called t channel, can bee seen on the figure.

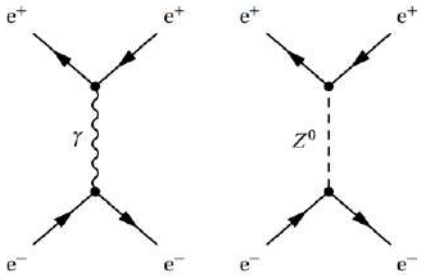

Figure 5: $e^+e^- \to e^+e^-$ (t channel), taken from [1].

An important difference of these channels is present in the dependence of the differential cross section on the angle:

$$\frac{\mathrm{d}\sigma}{\mathrm{d}\Omega} \propto \begin{cases} (1+\cos^2\theta) & s \text{ channel} \\ (1-\cos\theta)^{-2} & t \text{ channel} \end{cases} \tag{22}$$

[1]

On the Figure 6 and Figure 7 one can see the graphs of these dependencies.

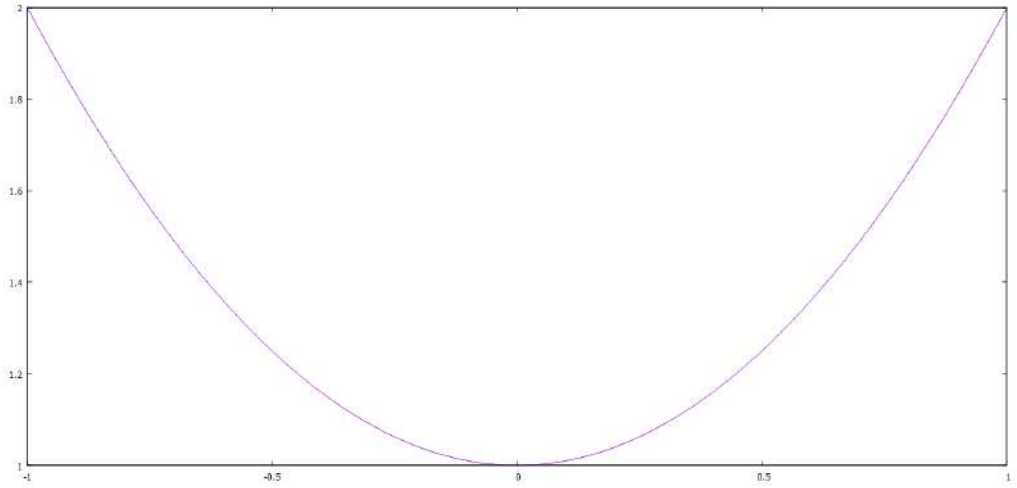

Figure 6: Angular dependence coefficient for s channel.

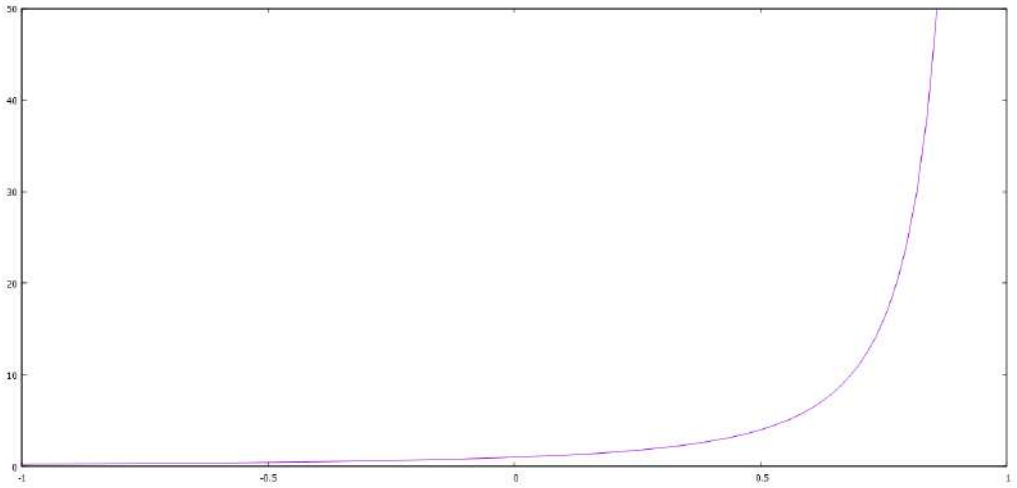

Figure 7: Angular dependence coefficient for t channel.

1.3 Experiment

1.3.1 OPAL detector

Here we will briefly present the OPAL detector that is used in the collider.

It contains central tracker, which detects trajectory of charged particles by magnetic field, electromagnetic calorimeter (ECAL), which can measure the energy of photons , electrons and

positrons, hadronic calorimeter (HCAL), measuring hadrons energies. In addition, there is also muon detector, however, we not consider it in our experiment. The scheme is shown on Figure 2.

The central tracker contains gas, passing through which a charged particle ionizes it, knocking out an electron, which then goes to the cathode, creating an electrical signal at the end. Taking into account all such signal from electrons, this allows one to establish the energy of the particle and its path in time, i.e. also the momentum.

In an electromagnetic calorimeter, secondary particles are created in the form of a cascade, in the presence of electromagnetic fields, so that secondary particles produce bremsstrahlung and Cherenkov radiation, which is detected by scintillators, information about which gives information about the initial energy.

In the hadron calorimeter, the creation of secondary particles occurs due to nuclear reactions after a collision with an iron material being detected, so similarly gives information about the initial particle energy.

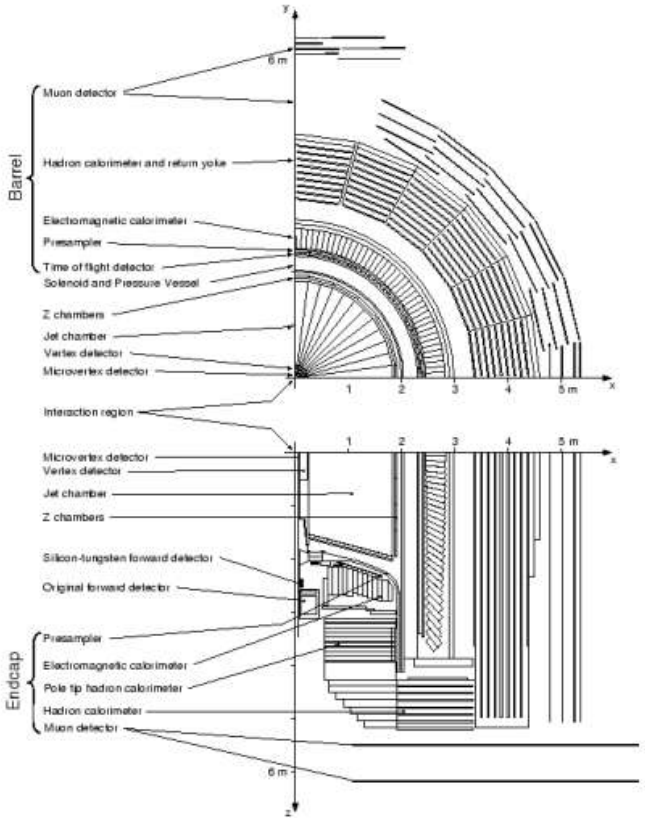

Figure 8: Scheme of the detector, taken from [1].

Also, to be able to calculated cross section, it is also necessary to measure the luminosity in the collider. It is done, measuring the events for the process with known cross section:

$$\int \mathcal{L} dt = \frac{N}{\sigma_{\text{known}}} \tag{23}$$

For more details see [1].

1.3.2 Cutting data

One of the most important thing in the analysis of the experimental data is the separation of data corresponding to different phenomena.

In particular, some processes could be classified by the total energy deposition difference, measured in ECAL and HCAL.

The key task in selecting a data type is the optimal choice of cut so that the number of desirable events is maximum and the number of undesirable events is maximum. For example, in one case, a high percentage of the desired events will be important to us, for which it is worth reducing the selected cutting size, and in another case, the number of desired events may be important to us, so the cutting size should be increased.

This can lead to problems, for example, when measuring the scattering cross section, the number of events is fundamentally important and may have a large error, while integrated luminosity is well known.

The solution could be to use the Monte Carlo method. In short, this is a simulation of the data, so we know more about it than the real data and can develop the cutting approach. However, it is important that the method does not strongly correlate with the theoretical assumptions in the simulation, because then everything will rest on them.

[1]

1.3.3 Plan

Here we briefly describe the plan of our laboratory work.

First, we need to find the classification criteria for separating e^+e^-, $\mu^+\mu^-$, $\tau^+\tau^-$, $q\bar{q}$ channels. For this we deal with pre-selected data sets (20 events in each dataset) from the OPAL using graphical display GROPE.

Second, we check our criteria using Monte-Carlo generated data (with the scale about 10000 events in one dataset). We obatin the efficiency of the cutting method and background.

Finally, we work with the data from the OPAL detector (also the scale is 10000 events in one dataset). By analyzing these data, what we will do next, some properties of the Z^0-boson can be elucidated.

2 Experiment

2.1 Classification rules with simulated data

2.1.1 Variables

Here we preset the simulated data, with a help of similar to which data we determine the selection criteria and their validity for different process outcomes. Below are photos of the computer screen with this data visualization using GROPE (similar to the real collider):

Figure 9: The results of the collision of an electron and a positron in the form of two electrones and muons correspondingly.

Figure 10: The results of the collision of an electron and a positron in the form of two tau particles and quarks correspondingly.

Not going into deep details, we are interested in the following measured variables:

N_{charged} - number of charged particles measured in the central tracker.
P_{charged} - total momentum of charged particles measured in the central tracker.
E_{ECAL} - total energy of particles measured in the ECAL.
E_{HCAL} - total energy of particles measured in the HCAL.

2.1.2 Classification of final particles

Using simulated data (with 10^5 events each) graphs showing the dependence of number of events on our variables, we come to the following determination (e^-e^+, $\mu^+\mu^-$, $\tau^+\tau^-$ or $q\bar{q}$ final state) criteria:

e^-e^+: $N_{\text{charged}} < 6$, $E_{\text{ECAL}} > 8$
$\mu^+\mu^-$: $P_{\text{charged}} > 75$, $E_{\text{ECAL}} < 20$
$\tau^+\tau^-$: $N_{\text{charged}} < 5$, $20 < P_{\text{charged}} < 75$, $E_{\text{ECAL}} < 65$
, $q\bar{q}$: $N_{\text{charged}} > 6$, $E_{\text{ECAL}} < 80$

It was obtained by eye, using graphs as on Figure 8, which is an example for the E_{ECAL} variable. The key idea was to isolate the majority of the type of interest and keep the least possible number of the other three types.

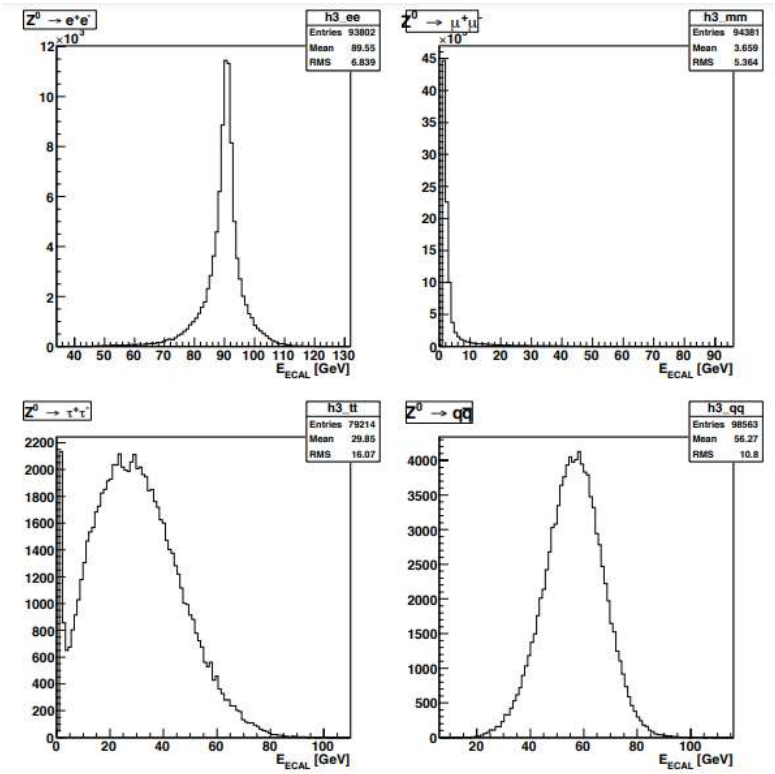

Figure 11: Simulated date plots showing dependence of number of events on E_{ECAL} for three considered final particle states.

An important concept for describing the reliability of criteria while applied to the data is the so-called efficiency matrix. Its rows correspond to the criteria used, and their intersections with columns determine how many events were classified accordingly. Its values, strictly speaking, are fractions (percentages), however, just numbers of events are also used as a quantity without normalization in the form of division by the total number of events, than it is coled non-normiled matrix.

Using simulated data with 10^5 events, we get the following values for this matrix (as the number of charged particles):

	e^-e^+	$\mu^+\mu^-$	$\tau^+\tau^-$	$q\bar{q}$
e^-e^+	86760	1	130	2
$\mu^+\mu^-$	0	85398	295	4
$\tau^+\tau^-$	151	2832	69453	29
$q\bar{q}$	1	0	974	96794

Table 1: Non-normalized efficiency matrix for classification of particles type.

2.1.3 Angle cutting

Since, as described earlier, for the case e^-e^+ we are interested only in s channel, we need cutting rule to filter it from t channel. We base this on their different dependence of differential cross section on the angle. See the Figure 9 on which is a screenshot from them computer with a graph.

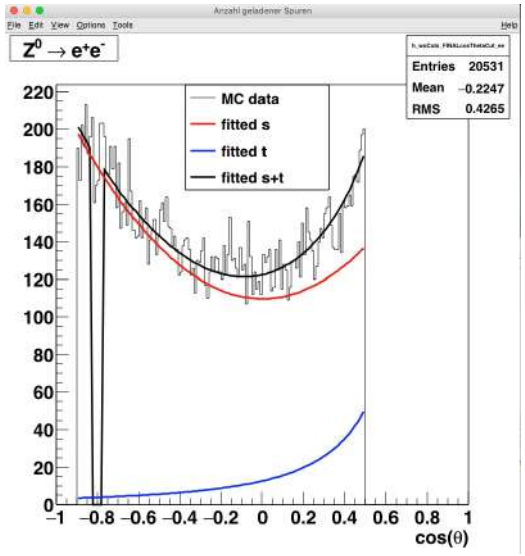

Figure 12: Differential cross section dependence of $e^-e^+ \rightarrow e^-e^+$ on cosinus of the angle, experimental data for both s and t channel, fitting curves for each of them.

Our choose for cutting criteria is to take $\cos\theta$ from -0.9 (this is done to avoid background noise) to 0.5 (this choice is made in accordance with the dependencies, by eye) .

Next, we use this criterion both with the selection criteria for the e^-e^+ case. Therefore, we need to modify the efficiency characteristic due to this new rule .

We again deal with the simulated data which consists 10^5 events. Consider $N_{s\,\cos}$ as number of filtered events using cos cutting criteria which in fact are s accepted channels events. Then, taking into account the differential cross section formula, whole number of s channel events can be estimated as:

$$N_s = N_{s\,\cos}\frac{\int_{-1}^{1}(1+\cos^2\theta)\,\mathrm{d}\cos\theta}{\int_{-0.9}^{0.5}(1+\cos^2\theta)\,\mathrm{d}\cos\theta} \tag{24}$$

This, final efficiency for e^-e^+ , e^-e^+ element, , could be defined as

$$E_{e^-e^+\,,e^-e^+} = \frac{N_{\text{passed total}}}{N_s}, \tag{25}$$

where $N_{\text{passed total}}$ is total number after using both filter criteria. According to our values received using the code on the computer, $N_{s\,\cos} = 20531 \times 0.91$, $N_{\text{passed total}} = 20144$.

This lead to the following final efficiency matrix (normalized):

$$E_{ij} = \begin{pmatrix} 0.79706 & 0.00001 & 0.00130 & 0.00002 \\ 0 & 0.85398 & 0.00295 & 0.00004 \\ 0.00151 & 0.02832 & 0.69453 & 0.00029 \\ 0.00001 & 0 & 0.00974 & 0.96794 \end{pmatrix} \tag{26}$$

2.2 Real data

2.2.1 Expression for errors

According to the definition of the efficiency matrix, we expect the following relation between real (expected) numbers (vector index corresponds to classification type) of events and measured (filtered):

$$\vec{N}_{mes} = \hat{E}\,\vec{N}_{real} \tag{27}$$

This leads to the following expression for the total cross sections, in which we are interested in:

$$\vec{\sigma} = \frac{\hat{E}^{-1}\vec{N}_{mes}}{L} \tag{28}$$

Here L is integrated luminosity during the time of collision, which is known.

To analyze the data, we need to obtain expressions for the errors. For total error we write:

$$\Delta\vec{\sigma} = \sqrt{\left(\frac{E^{-1}\vec{N}_{\text{cut}}\Delta L}{L^2}\right)^2 + \left(\frac{E^{-1}\Delta\vec{N}_{\text{cut}}}{L}\right)^2 + \left(\frac{\Delta E^{-1}\vec{N}_{\text{cut}}}{L}\right)^2} \tag{29}$$

ΔL is known from the data, while other erros need to be determined.

As initial assumption, for every measured number N we estimate its error as $\sqrt{N}$. Describing each element of the matrix E_{ij} as $\frac{N_{filtered}}{N_{filtered}+N_{other}}$, where $N_{filtered}$ is number of passed events and N_{other} is $10^5 - N_{other}$, considered here as independent variable, one can come to the following error formula:

$$\Delta E_{ij} = \sqrt{\frac{E_{ij}(1-E_{ij})}{10^5}} \tag{30}$$

To obtain the error of E^{-1} we expand its definition up to first order as

$$(E + \Delta E)(E^{-1} + \Delta E^{-1}) = \Delta 1 = 0 \tag{31}$$

and get (up to sign):

$$\Delta E^{-1} = E^{-1} \Delta E E^{-1} \tag{32}$$

Thus, we have all the criteria and errors that we build into our real data analysis.

2.2.2 Results

Using our efficiency matrix and formulas, obtained for cross section and its error, with help of the computer code, we calculate the cross sectiones for the real data from the collider.

In the Figure 13, one can see the scattering cross sections near the peak obtained as a result of data analyses. Fitting curve here is Breit-Wigner distribution:

$$y(x) = p_0 \left(\frac{4\,(x - p_1)^2}{p_2^2} + \left(\frac{x}{p_1} \right)^2 \right)^{-1} \tag{33}$$

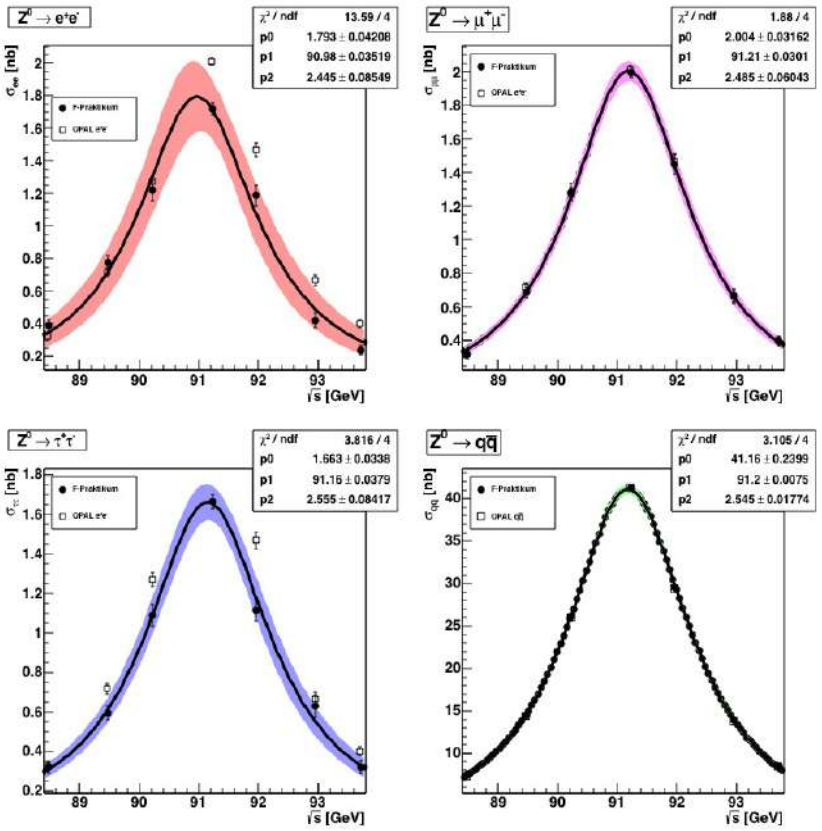

Figure 13: Cross section dependence for e^-e^+, $\mu^+\mu^-$, $\tau^+\tau^-$, $q\bar{q}$ final state. Black points correspond to our analysis of the data, while white points are known OPAL data. χ is chi-square characteristic of the fitting.

We can see that the first fitting is a bit bad, the second is good, while the third and the fourth are acceptable, but not perfect. The leading reason for the first one seems to be non ideal angle cutting, in particular, some deviation es for energies higher than the peak. While reason for the others is quite rough rule for selection of types.

However, in general all the results can be considered as acceptable and we use them in our analysis.

3 Analysis

3.1 Resonance parameters

First, we are interested in determining Z^0 boson mass and related decay widths.

Using theory described in the preparation section, in particluar formula for the peak cross section, it is not hard to understand that the mass of the Z^0 corresponds here to the parameter p_1.

We calculate it as a so-called weighted average:

$$\bar{M_{Z^0}} = \frac{\sum p_{1i}(\Delta p_{1i})^{-2}}{\sum_i (\Delta p_{1i})^{-2}} \pm \sqrt{\frac{1}{\sum_i (\Delta p_{1i})^{-2}}} = 91.190 \pm 0.007\text{GeV} \tag{34}$$

Comparing it with [3] where $M_{Z^0} = 91.1876(21)$GeV, we conclude that the result is correct within the error.

By analogy, weighted average of Γ_Z, corresponding to the p_2:

$$\bar{\Gamma}_Z = 2.537 \pm 0.016\text{GeV} \tag{35}$$

Comparing it with the theoretical value $\bar{\Gamma}_Z = 2.4862$GeV calculated in our preparation, we see that the deviation is a bit bigger that error bar.

Also we can determine the life time of the Z^0 boson:

$$\tau = \frac{\hbar}{\bar{\Gamma}_Z} = (2.594 \pm 0.016) \times 10^{-25}\text{s} \tag{36}$$

Comparing with the value calculated in the preparation (2.6475×10^{-25}s), wee see that there is also some deviation.

Using formula for σ_f, determined in the preparation, and dealing with the erros according to the usual rules, we get:

$$\Gamma_e = 50.47 \pm 1.51\text{MeV}\ ,\ \Gamma_\mu = 56.41 \pm 1.29\text{MeV},$$
$$\Gamma_\tau = 46.81 \pm 1.26\text{MeV}\ ,\ \Gamma_q = 1171.03 \pm 18.51\text{MeV} \tag{37}$$

Comparing these values with the calculated from the known data $\Gamma_e = \Gamma_\mu = \Gamma_\tau = 83.8$MeV,$\Gamma_q = 1732$MeV, which are obtained using data from Figure 4, we can conclude that, unfortunately, they deviate by much more than the error bars.

3.2 Number of neutrinoes

According to the described theory, in the process of the Z^0 boson decay light neutrinoes ($m_\nu < \frac{1}{2} M_{Z^0}$) also being created. And their number can be calculated as

$$N = \frac{\Gamma_Z - \Gamma_e - \Gamma_\mu - \Gamma_\tau - \Gamma_q}{\Gamma_\nu} = 7.23 \pm 0.11, \tag{38}$$

where we use values from the last results for Γ_e, Γ_μ ,Γ_τ, Γ_q, $\bar{\Gamma}_Z$ together with $\Gamma_\nu = 167.6$MeV from the Figure 4.

While using the theoretical data from the Figure 4, we expect it to be $N = 3$. Thus, unfortunately, we also have here deviation by more than the error bar.

4 Conclusion

In this experimental work we were able to analyse the data from OPAL detector consists of colliding positron and electron and determine peak cross sections for different final particles, with the help of which we calculated related decay widths and got mass and lifetime of the Z^0, number of neutrinos in the process.

Our result of Z^0 mass is fully with agreement with the expected value. (our value is 91.190 ± 0.007GeV, expected is $M_{Z^0} = 91.1876(21)$GeV), while the total decay width there is deviation bigger than the error, same as for the life time (our values: $(2.594 \pm 0.016) \times 10^{-25}$s, 2.537 ± 0.016GeV expected: 2.6475×10^{-25}s, 2.4862GeV). However, these results are quite close.

The obtained partial decay widths, unfortunately, differs from the expected quite a lot (our values: $\Gamma_e = 50.47 \pm 1.51$MeV, $\Gamma_\mu = 56.41 \pm 1.29$MeV, $\Gamma_\tau = 46.81 \pm 1.26$MeV, $\Gamma_q = 1171.03 \pm 18.51$MeV, expected: $\Gamma_e = \Gamma_\mu = \Gamma_\tau = 83.8$MeV,$\Gamma_q = 1732$MeV)

Moreover, estimated number of neutrinoes is too big (our value: 7.23 ± 0.11, expected: 3).

In general, our results are qualitatively correct and we were able to see the physics, in which we were intersted in, but, unfortunately, the accuracy is not good enough.

It seems to be that the main cause of the errors and inaccuracies are our non-ideal data selection criteria. The cutting, especially for some types, was forced to be rather rough and we already see on the graphs of the cross section that the fitting is not perfect in corresponding places.

In particular, the accuracy of the experiment could be improved by using additional parameters for the cutoff (perhaps a muon detector) and a more thorough study of the cutoff characteristics based on a large amount of data (perhaps using artificial intelligence).

References

[1] Instructions to the Lab Experiment M48: Properties of the Z^0-Boson, Studon.

[2] https://en.wikipedia.org/wiki/Standard Model.

[3] C. Amsler et al. (Particle Data Group): Review of Particle Physics. Physics Letters B 667 (2008) 1; website: http://pdg.lbl.gov